Initial Arcuate Defects within the Central 10 Degrees in Glaucoma

Donald C. Hood,[1,2] *Ali S. Raza,*[1] *Carlos Gustavo V. de Moraes,*[3,4] *Jeffrey G. Odel,*[2] *Vivienne C. Greenstein,*[2,4] *Jeffrey M. Liebmann,*[3,4] *and Robert Ritch*[3,5]

Purpose. To better understand the relationship between the spatial patterns of functional (visual field [VF] loss) and structural (axon loss) abnormalities in patients with glaucomatous arcuate defects largely confined to the central 10° on achromatic perimetry.

Methods. Eleven eyes (9 patients) with arcuate glaucomatous VF defects largely confined to the macula were selected from a larger group of patients with both 10-2 and 24-2 VF tests. Eyes were included if their 10-2 VF had an arcuate defect and if the 24-2 test was normal outside the central 10° (i.e., did not have a cluster of three contiguous points within a hemifield). For the structural analysis, plots of retinal nerve fiber layer (RNFL) thickness of the macula were obtained with frequency-domain optical coherence tomography (fdOCT). The optic disc locations of the RNFL defects were identified on peripapillary fdOCT scans.

Results. The VF arcuate defects extended to within 1° of fixation on the 10-2 test and were present in the superior hemifield in 10 of the 11 eyes. The arcuate RNFL damage, seen in the macular fdOCT scans of all 11 eyes, involved the temporal and inferior temporal portions of the disc on the peripapillary scans.

Conclusions. Glaucomatous arcuate defects of the macula's RNFL meet the disc temporal to the peak of the main arcuate bundles and produce a range of macular VF defects from clear arcuate scotomas to a papillofoveal horizontal step ("pistol barrel scotoma"). If RGC displacement is taken into consideration, the RNFL and VF defects can be compared directly. (*Invest Ophthalmol Vis Sci.* 2011;52:940–946) DOI:10.1167/iovs.10-5803

Preserving central vision is of paramount importance in treating glaucoma. However, it is fair to say we know more about paracentral damage than we do about damage to this most important region for visual function. This is in part due to the fact that visual field (VF) damage is commonly assessed with standard automated perimetry (SAP) and the 24-2 test. The 24-2 test pattern has only four points within the central 4.2° (radius) of fixation and only one point within the fovea, which is optional. However, it is clear that the center of the visual field, including the fovea, can be affected by glaucoma,[1–7] even in early stages of the disease process.[3,5] Here we describe an approach for better understanding the structural changes associated with glaucomatous VF damage in the central 8 to 10°, which corresponds anatomically to the macula.

The number of glaucomatous, macular defects detected increases when a test pattern with a spatial grain finer than the typical 6° × 6° grid of the 24-2 is used.[3–6] While these VF defects in the macular region appear to take a variety of forms,[3,4] it is clear that an arcuate-shaped defect is commonly seen.[3–6] It is less clear how these macular VF defects relate to structural damage at the level of the retina and the optic disc. For example, are the clusters seen on the VF due to arcuate-like damage at the level of the retinal nerve fiber layer (RNFL)? And, what part of the disc shows RNFL damage in these patients? With the newer frequency domain optical coherence tomography (fdOCT) technology, the thickness of the retinal ganglion cell (RGC) layer and RNFL in regions of the macula can be measured. In general, the focus of fdOCT studies of the macula in glaucoma has been on the relative sensitivity of macular measures compared with measures of peripapillary RNFL thickness.[8] (See Ref. 8 for further references.) Wang et al.[9] recently reported that the RGC and RNFL thicknesses along the horizontal meridian could be depressed relative to controls in patients with glaucoma with or without abnormal foveal (fixation) sensitivity. However, this study used single fdOCT line scans and could not differentiate among alternative patterns of damage. In the present study, the macula and optic disc regions were scanned with multiple (volume) scan strategies. Sakamoto et al.[10] have recently shown that the RNFL thickness maps derived from fdOCT volume scans are effective in revealing macular RNFL defects.

Our purpose was to better understand the relationship between the spatial patterns of VF loss and structural RNFL abnormalities in patients with glaucomatous arcuate defects largely confined to the central 10° on achromatic perimetry.

Methods

Arcuate Patterns of Visual Field Abnormalities

Eleven eyes of nine patients with arcuate glaucomatous VF defects predominantly in the macular region were selected from a larger group of patients in the following way: Of 258 consecutive glaucoma patients or glaucoma suspects referred for mfVEP[11–15] testing over a 2-year period, 101 patients (168 eyes) had both 24-2 and 10-2 VF tests performed using the SITA-standard test strategy (Humphrey Visual Field Analyzer; Carl Zeiss Meditec, Inc, Dublin, CA).

From the Departments of [1]Psychology and [2]Ophthalmology, Columbia University, New York, New York; the [3]Department of Ophthalmology, Manhattan Eye, Ear & Throat Hospital, New York, New York; the [4]Department of Ophthalmology, New York University, New York, New York; and the [5]Department of Ophthalmology, New York Medical College, Valhalla, New York.

Supported by National Eye Institute Grant R01-EY-02115, Glaucoma Research and Education Fund of Lenox Hill Hospital, NY, NY (CGVdM); and the James Cox Chambers Research Fund of the New York Glaucoma Research Institute, NY, NY.

Submitted for publication April 29, 2010; revised August 16, 2010; accepted September 6, 2010.

Disclosure: **D.C. Hood**, Topcon Inc. (F, C); **A.S. Raza**, None; **C.G.V. de Moraes**, None; **J.G. Odel**, None; **V.C. Greenstein**, None; **J.M. Liebmann**, Topcon, Inc. (F, C); **R. Ritch**, None

Corresponding author: Donald C. Hood, Department of Psychology, 406 Schermerhorn Hall, Columbia University, New York, NY 10027; dch3@columbia.edu.

Because our focus here was on VF damage largely in the macula, in addition to excluding patients with an unreliable 10-2 and/or 24-2 VF (fixation rate >33% or false positive/negative rates >20%), we also excluded those with defects outside the central 10° on the 24-2 test. In particular, eyes were excluded if their 24-2 test had a cluster of three contiguous points (5%, 5%, 1%) within a hemifield, but outside the central 10°. That is, the cluster could not cross the horizontal midline and could not include the 12 points falling within the central 10°, within the hatched region in Figure 1, which shows a 24-2 VF that met our criteria for inclusion. Twenty-seven eyes met these criteria.

For these 27 eyes (22 patients), the 10-2 VF was abnormal in 16 eyes (14 patients). A 10-2 VF was considered abnormal if it satisfied the same cluster criterion used for the 24-2 test or if the 10-2 MD had a P value < 0.05. The 11 eyes (11 patients) with normal 10-2 VFs were not studied further.

Because we were interested in arcuate defects, the VF of the 16 eyes with abnormal 10-2 fields were classified as arcuate (12 eyes) or "other" (four eyes) using the following criteria: Arcuate VF defects were defined based on the appearance of the abnormal locations on the 10-2 test. Based on the characteristics of classic glaucomatous arcuate field defects, to be classified as an arcuate on the 10-2, the abnormal region had to follow an arc, include abnormalities in the nasal field, and had to be closer to fixation nasally than temporally. (See Figs. 2 and 3 and the Results for further details.) One eye with an arcuate was excluded as we were unable to obtain a fdOCT test within 12 months of the 10-2 test. Although the analysis was performed on a single 10-2 VF test, of the 11 eyes with arcuate defects, nine had repeat 10-2 tests, with all nine confirming the arcuate defect. In addition, the mfVEP tests (not shown) also demonstrated abnormal regions consistent with these scotomas in all 11 eyes. The 11 eyes were classified as normal-tension (eight), POAG (two), and exfoliative (one) glaucoma. The refractive errors ranged from −5.50 to +2.00 DS for these eyes.

Of the four eyes classified as "other," two had diffuse loss on the 10-2 VF and depressed RNFL thickness throughout the central retina both on the 3D scans and on the peripapillary RNFL thickness profiles. A third eye was probably normal; the mfVEP and fdOCT results were normal, as was the RNFL profile from the peripapillary scan. In addition, the 10-2 test of this patient, performed during a recent return visit, was normal. The 10-2 test of the fourth eye showed largely a temporal field abnormality that was undoubtedly due to an old vascular occlusion. The associated lesion could be seen as a local thinning of the inner layer and inner plexiform layers, as well as the RGC and RNFL layers, on the fdOCT.

Written informed consent was obtained from all participants. Procedures followed the tenets of the Declaration of Helsinki and the protocol was approved by the Committee of the Institutional Board of Research Associates of Columbia University.

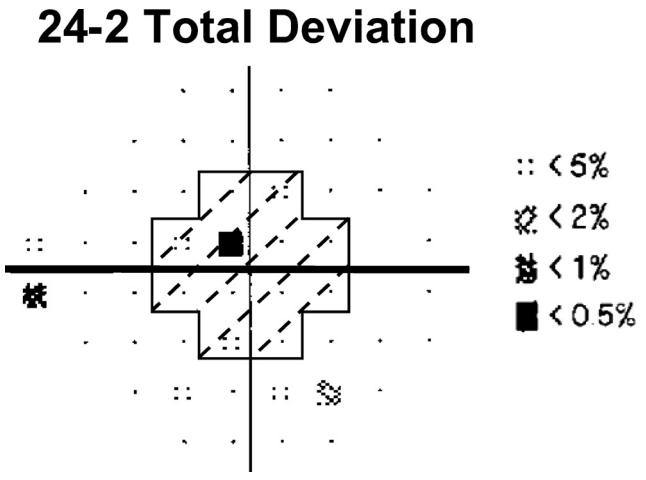

FIGURE 1. The 24-2 test pattern showing the region (*dashed diagonal lines*) represented by the 10-2 test pattern. Patients were excluded if their 24-2 had a significant cluster (5%, 5%, or 1%) of points outside this region, but within a hemifield.

OCT Testing

To better understand the structural bases of the 10-2 defects, fdOCT scans (3D OCT-1000, Topcon, Paramus, NJ) were examined. Of the 11 eyes meeting the inclusion criteria, six eyes had fdOCT scans within 1 month of the 10-2, while only one had a time between the fdOCT and 10-2 VF that exceeded 6 months. However, the scan of this eye (Patient 7) was obtained 11 months before the 10-2 VF and even at that point in time an arcuate can be seen on the scan (Fig. 3A).

The 3D cube (volume) scans (over a 6 by 6 mm region, 128 horizontal B-scans with 512 A-scans each) were obtained using both macula and optic disc fixation targets. The RNFL thickness was determined by the machine's software. For the macula, RNFL thickness from the cube scan was displayed as a pseudocolor map (second and fourth columns in Figs. 2 and 3). The quality score (Q) for these scans was 63 ± 12. However, the scans were not chosen based on Q score as we were interested in the integrity of the macular cube scan. We avoided scans with signs of possible eyelid occlusion or lateral eye movements, regardless of the Q score. For the peripapillary region, the information from the optic disc cube scan was displayed as a RNFL profile around a circle of 3.4 mm diameter centered by the operator on the optic disc (Fig. 4A).

Terminology

When labeling defects, one must be careful to distinguish between the topographical shape of the defect (i.e., VF loss) on the VF and the topographical shape of the defect (i.e., RNFL thickness) on the retina. For example, we will refer to "arcuate VF defects" to refer to the former and "arcuate RNFL defects" to refer to the latter. As illustrated below, an arcuate RNFL defect may or may not produce a VF defect that appears as an arcuate scotoma.

RESULTS

Eleven eyes (nine patients) show an arcuate VF defect, as defined above, inside the central 10°. These arcuate defects were largely confined to the central 10-2, as by definition they did not have a significant cluster of points outside the central 10° on the 24-2 VF. Figures 2 and 3 show the total deviation plots for the 10-2 and the fdOCT RNFL thickness plots for these 11 eyes. Note that in Figures 2 and 3, all test results for the left eyes were reversed along the vertical midline to appear as if they were right eyes. That is, on all plots the nasal field (temporal retina) is to the left and the temporal field (nasal retina) to the right.

Arcuate Patterns of Visual Field Abnormalities

Of these 11 eyes, nine (Figs. 2 and 3C) showed a clear arcuate on the 10-2 test. These arcuates stretched from the midline in the nasal field to the edge of the temporal field. The 10-2 VF of the other two of these 11 eyes (Figs. 3A,B) were "incomplete arcuates" in the sense that the abnormal points were largely in the nasal field. Further, 10 of these 11 arcuates were in the superior hemifield. The exception, patient 9 in Figure 3C, deserves special note. We classified the lower field as an arcuate. However, we argue below that there are two separate defects in the upper field as well.

Arcuate Patterns of RNFL Abnormalities

The fdOCT RNFL thickness plots of Figures 2 and 3 were examined for arcuate defects. In these RNFL plots, the lighter colors represent thicker and the darker colors thinner RNFL as shown by the calibration bar in Figure 3D. There was thinning of the RNFL (red arrow) consistent with an arcuate RNFL defect in

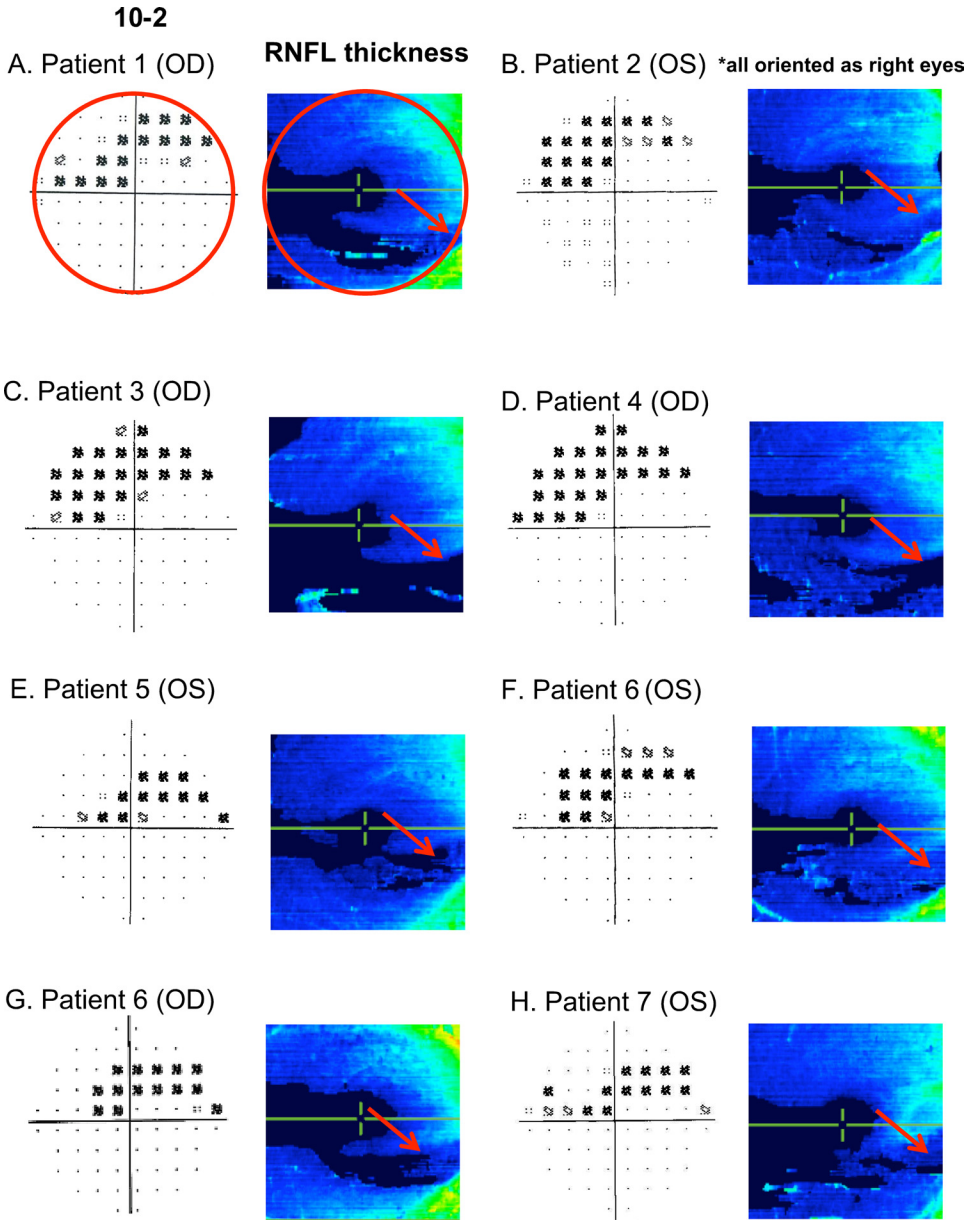

Figure 2. (**A–H**) The results of eight eyes with complete arcuate defects on the 10-2 test. For each panel, the columns show the results for the 10-2 test (*left*) and fdOCT RNFL thickness analysis (*right*). For the RNFL thickness plot, the code is shown as the color bar in Figure 3D.

all 11 eyes. Note that in the case of patient 9 (Fig. 3C) mentioned above, in addition to confirming the arcuate damage in the lower field (red arrow in the superior retina), there is evidence of a similar defect in the upper field/lower retina on both the 10-2 and RNFL plots (green arrows). (Note that part of this arcuate is obscured in the RNFL plot by the dark orange semi-transparent region. This is to indicate that the algorithm failed in this region and the plot cannot be trusted. There were missing data due to light occlusion by the eyelid.) The defects on the fdOCT were confirmed on the RNFL plot in the right most panel of Figure 3C obtained 8 months later. In any case, in addition to these arcuate defects, there is a horizontal step scotoma in the temporal VF just above the midline (orange arrow). The RNFL defect associated with this papillofoveal horizontal step abnormality on the VF appears to be an arcuate RNFL thinning as shown by the orange arrows in Figure 3C (right-most panels). The orange arrows indicate the edges of an arcuate that starts close to the fovea and extends to the disc. Consistent with this structural defect is the observation that this VF defect on the 10-2 does not include the foveal center (sensitivity: 37 dB), even though this defect is very deep, −16 to −25 dB for the 5 VF points involved. An anatomic explanation for this finding will be proposed in the Discussion.

Characterization of the Arcuate Defects

The data from these 11 eyes were further analyzed to better understand the nature of these arcuate defects. For the purpose of this analysis, we excluded the defects in the superior field of patient 9 (Fig. 3C), so that only one defect was included per eye.

First, consider the location of these 11 arcuate defects on the VF. On the nasal side of the field, in eight eyes the defect extended to the closest point tested (−1°,1°); that is, within 1.4° of the foveal center. The nasal location of the largest VF loss was between this point and the 5° point in 10 of the 11 eyes. Thus, deep arcuate defects occur in and near the foveal region of the VF. Figure 5 shows the median total deviation on the 10-2 test for the eight eyes with the clear upper VF arcuates in Figure 2. The region included within the black borders includes the points with a median deviation ≤−9 dB. Inspection of the abnormal regions of the 10-2

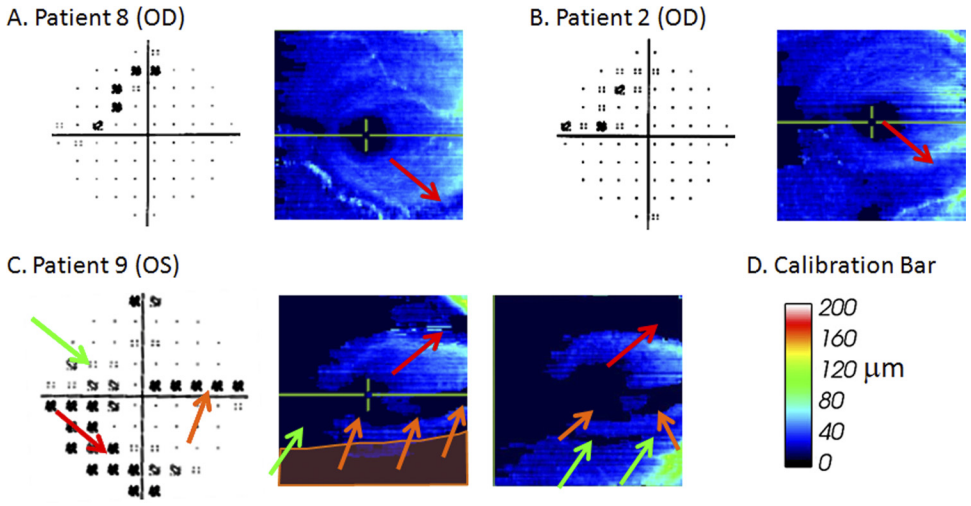

FIGURE 3. (**A**–**C**) Same as in Figure 2 for 3 patients with partial arcuates on the 10-2 test. For the RNFL thickness plot, the code is shown as the color bar in (**D**).

VFs in Figure 2 indicates that they often included this region.

Second, we also examined the location of the RNFL damage near the disc using the peripapillary volume scans. We were able to identify a marked thinning in the peripapillary RNFL profile of all 11 eyes with arcuate defects. For example, see Figure 4A, where the arrow marks the minimum of a dip in the RNFL thickness. Figure 4B shows the RNFL thickness plot from the scan of this patient's macula superimposed on a photograph of the patient's fundus. The blue circle is the approximate location of the circle scan associated with the RNFL profile in Figure 4A. The red dot shows the location of the dip. Notice that it corresponds to the arcuate RNFL thinning seen on the fdOCT scan. For the 10 eyes with an upper VF arcuate defect, the location of the dip (arrow in Fig 4A and red dot in Fig. 4B) fell within a relatively narrow range, 295° to 322°, as indicated by the red lines on the blue scan circle in Figure 4B. For comparison, the green bars show the range, 257° to 295°, of the peaks in the RNFL profiles of 16 controls with normal vision.[16] The point of maximal thinning associated with these RNFL arcuates is located adjacent to the peak of the classic arcuate bundles, suggesting the damage fibers should be considered part of these bundles.

Finally, seven (six patients) of the 11 eyes (Figs. 2A, 2D–H, and 3A) had evidence of a hemorrhage in the region of the disc associated with the RNFL defect. Local hemorrhages have long been associated with arcuate defects close to fixation.[17] Further, glaucomatous VF defects can precede the disc hemorrhage and the underlying RNFL damage associated with these defects has been hypothesized to be the cause of the hemorrhage in such cases.[18] In six of our seven eyes with hemorrhages, VF defects occurred earlier than did the disc hemorrhage.

DISCUSSION

Our purpose here was to better understand the nature of the RNFL damage due to glaucoma associated with arcuate VF defects largely restricted to the macular region. Eleven eyes with arcuate defects on the 10-2 VF tests, but with relatively normal 24-2 tests outside the 10° region examined by the 10-2 test, were studied. All 11 of these eyes showed arcuate-like damage to the RNFL on the fdOCT scans.

The peripapillary RNFL damage in these 11 eyes was located on the temporal side of the inferior temporal bundle of fibers. The location of the RNFL thinning suggests that the damaged fibers are contiguous with, and in some cases part of, the classically defined arcuate RNFL bundles even though the VF defects can be seen within 1° of fixation. This supplies a structural basis for why the macular arcuate VF defects seen here, and scattered throughout the literature[3–6,17] share characteristics with the classic arcuate scotomas seen on 24-2 testing. For example, classic arcuate scotomas, including those that extend into the central 10°,[6] are more often seen in the superior hemifield.[6,7,19] In the present study, only one eye had an inferior VF defect and even in this case we argued that the superior hemifield showed arcuate defects as well. In addition, as with the classic VF arcuate scotomas, the macular arcuate scotomas typically included the most nasal portions of the VF.

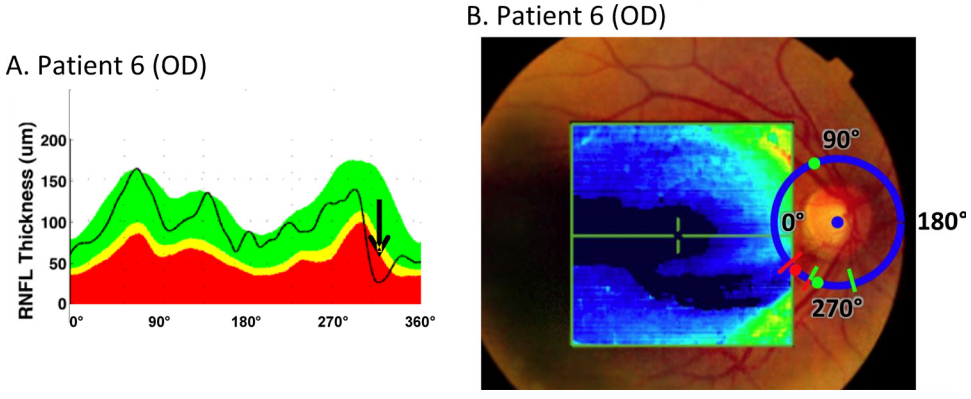

FIGURE 4. (**A**) RNFL profile (*black curves*) from fdOCT optic disc volume scan for the right eye of patient 6. The *colored* regions code the confidence intervals from control values. The *arrow* shows the dip in the RNFL profile associated with the VF defect. (**B**) The pseudocolor RNFL thickness plot for the same eye superimposed on the patient's fundus photograph. *Blue circle*: the locus of points represented in (**A**). *Red dot*: the location of the dip in (**A**). For the RNFL thickness plot, the code is shown as the color bar in Figure 3D.

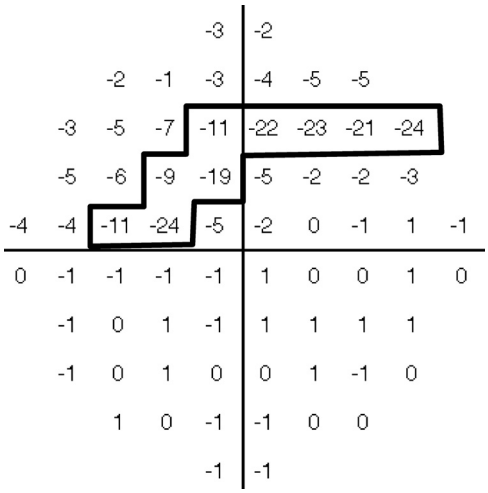

FIGURE 5. Median total deviation for the 10-2 tests of the eight patients in Figure 2 with superior field arcuate scotomas.

A Schematic for Relating Structural and Functional Arcuate Damage

To better understand the relationship between the RNFL damage and the macular VF defects, the schematic in Figure 6A (right panel) was developed. The schematic depicts a fundus view of the right eye. The structures in black were drawn to scale (see 5° bar on figure). The small bold circle is the RGC free foveal center, measured anatomically to be approximately 0.5° in radius,[20] while the gray dashed circle is the approximate border of the foveal depression, which is approximately 2.4° in radius.[21] In this schematic, the optic disc is shown as a 3° radius circle centered at an angle of 6.3° above the horizontal meridian (thin dashed orange line) and 15.6° from the foveal center; these represent average values from the literature.[22,23] Of course, the values for individuals will vary. For example, the location of the disc in relation to the fovea shows variation among individuals.[22,23]

It is important to distinguish between the location of the receptors onto which the retinal image of a 10-2 test spot falls and the location of the RGCs activated by those receptors. This is particularly important close to the fovea as the RGCs associated with this region are displaced the most. To illustrate this distinction, consider the 16 test points shown as the colored symbols in the 10-2 VF (upper left panel). On the schematic in the right panel, the small open symbols are the locations of the retinal images of these 16 test points. (Note that the actual test points are smaller than indicated.) The RGCs innervated by light falling at these points are displaced by progressively greater amounts as the foveal center is approached. Drasdo et al.[20] measured this displacement in postmortem human tissue. Using their information, we estimated the average location of the RGCs associated with the receptors located at each of the test spots. These locations are indicated by the larger filled symbols. (Note that the size of these symbols has no meaning here.)

The schematic can be used to illustrate the arcuate nature of the defects at the level of the RGC/RNFL. The left panel in Figure 6B is from Figure 5. The purple lines in the right panel were drawn to include the filled symbols corresponding to the symbols within the purple borders on the VF (left panel). The lines were extended to terminate at the disc in the middle of the red diagonal lines. Recall from Figure 4B that this is the region of the disc showing the range of minimum RNFL thicknesses associated with 10 superior VF arcuates.

While Figure 6B provides an anatomic basis for the "typical" or median central arcuate seen here (Fig. 5), it does not explain the horizontal step defect seen on the 10-2 VF of Patient 9 (orange arrow in Fig. 3C, left panel) and reproduced as the region enclosed within the purple borders of Figure 6C (left panel). The purple borders in Figure 6C (right panel) were drawn to indicate how an arcuate RNFL defect can include the abnormal points within the purple borders of the left panel. By this analysis, this papillofoveal horizontal step on the VF is, in fact, due to a very "tight" arcuate defect in the RNFL. As Lawton-Smith called tight arcuates on the VF "pistol" defects (see his comment on page 118 in Ref. 17), this could be called a "pistol barrel" defect. In any case, the arcuate of RGC/RNFL damage associated with this pistol barrel extends on the retina from the RGCs at approximately 3°, associated with the test spot at approximately 1°, to the inferior temporal region of the disc. This path of the hypothesized RNFL defect in Figure 6C resembles the pattern of RNFL thinning seen in Figure 3C (orange arrows in right panels).

Thus, arcuate RNFL defects seen in glaucoma can produce VF defects that range from a papillofoveal horizontal step, which resembles a pistol barrel, in the temporal field to the classic arcuate scotomas easily identified on the 24-2 test. To locate the approximate disc position of the classic arcuate scotomas on the schematics in Figure 7, note the blue, gray and red regions on the disc (right side of schematics). These correspond to the Garway-Heath et al.[24] superior temporal (blue), temporal (gray), and inferior temporal (red) regions of the disc, respectively. According to the Garway-Heath et al. map, the red region of the disc (inferior temporal) corresponds, on average, to a region (superior hemifield arcuate) on the 24-2 from approximately 6° to ≥27°. In terms of the location of the RGCs, this corresponds to approximately 7.5° (the black circle in Fig. 6) to ≥27°. Thus, the arcuates in our study extend from inside the inferior arcuate region of the disc (red), as defined by Garway-Health et al., to within their temporal region (gray). Of course, there is variation among normal controls in mapping.[24,25] It remains to be seen how much of the variation among controls can be accounted for based on variation in the relative positions of the fovea and disc.

Implications

First, our results reinforce the importance of performing a test with a finer spatial grid if there is any evidence/concern about central damage.[5,6]

Second, while there is generally good agreement among abnormalities seen on macular OCT scans and 10-2 SAP total deviation plots,[22] the anatomic displacement of the RGCs needs to be considered for a full understanding. For example, arcuate-like RNFL defects may or may not appear as arcuate-shaped abnormalities on the VF; it will depend on the relative location of the damaged RGC region and the 10-2 test points. Further, the displacement of macular RGCs should be taken into consideration when using RNFL defects to map the points on the 10-2 test, or the central few points on the 24-2 test, to regions of the optic disc.

Third, and perhaps most important, Figure 6 suggests a way to combine visual field and fdOCT information so that the glaucoma specialist can see at a glance how the VF and RNFL defects do or do not agree. To illustrate this point, consider Figure 7. The 10-2 VF and RNFL thickness map are from Figure 2F (patient 6), along with this patient's RNFL thickness map for the 3D peripapillary scan. The RNFL maps are shown centered on the fovea and optic disc. The schematic from Figure 6A has been superimposed. This patient was chosen for this example because the relative location of the disc and fovea was close to that of the schematic in Figure 6, which was based on mean

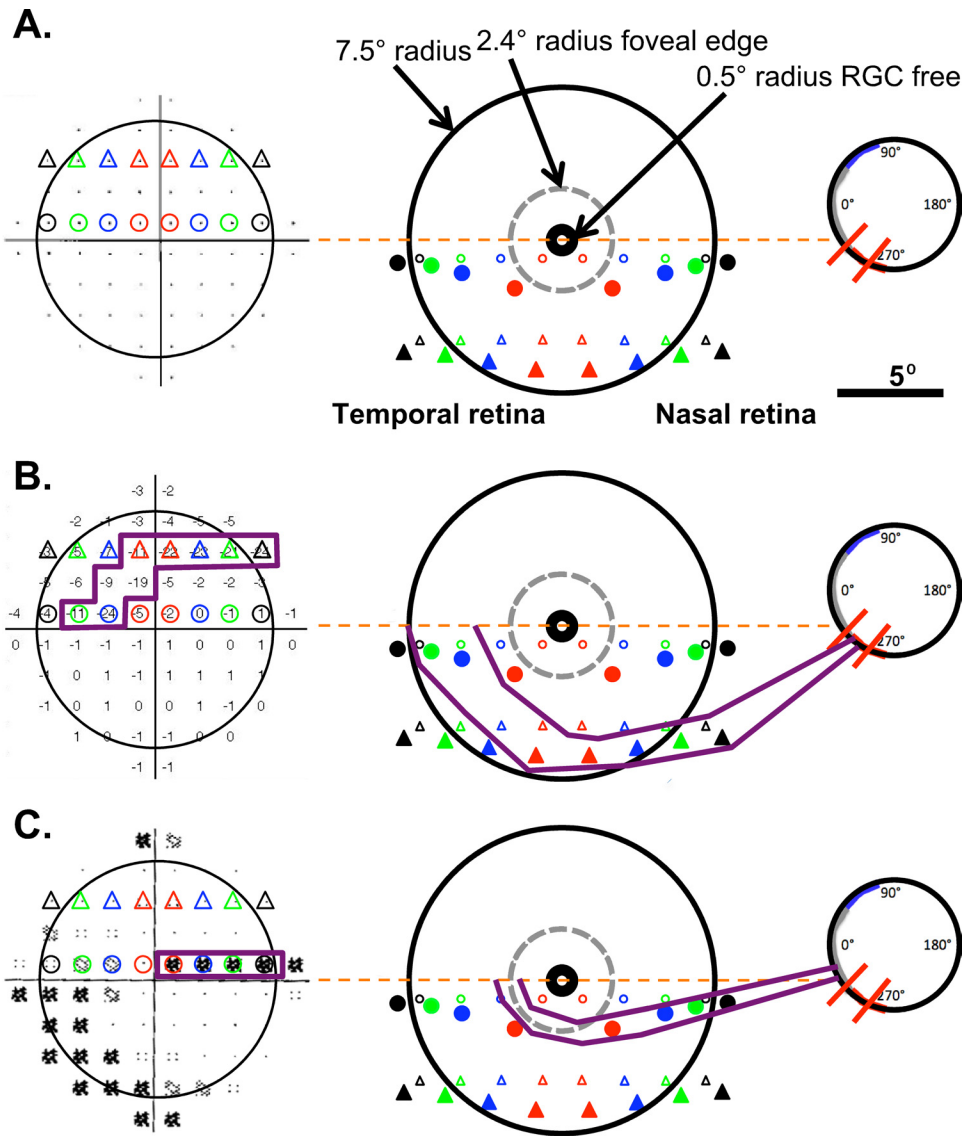

FIGURE 6. **(A)** The locations of the test spots on the 10-2 (*open symbols, left*) are shown on a schematic representation of the fundus view of the retina (*small open symbols*, *right*). The *filled symbols, left* show the location of the associated RGCs after taking the displacement of these cells into consideration. **(B)** Same as in **(A)** with the borders shown for the defect seen on the median plot in Figure 6. **(C)** Same as in **(B)** but for the cecocentral defect seen in patient 9 (Fig. 3C).

values from the literature. The solid red borders on the RNFL maps were derived from the 10-2 VF (right panel) and extended to the disc as the red and black lines using the procedure described above for Figure 6. At a glance, one can see that the RNFL thinning agrees with the red borders predicted from the visual field. We suggest that plots such as these might help the specialist identify glaucomatous damage, especially in cases of subtle field damage.

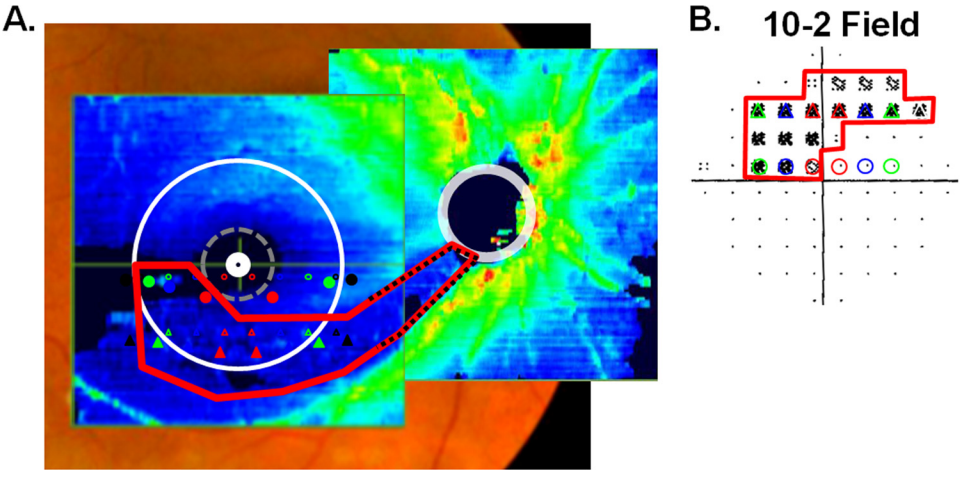

FIGURE 7. **(A)** The schematic representation from Figure 6A is superimposed on the fundus photo and RNFL thickness maps of patient 6 (Fig. 2F). The region within the *red borders* is the portion of the RNFL that is predicted to be abnormal based on the VF in **(B)**. **(B)** The 10-2 VF of this patient with the abnormal points outlined in *red*.

Finally, the analysis in Figures 6 and 7 opens the possibility that the relative position of the fovea and disc may contribute to the risk of macular damage. In particular, patients in whom the RGC fibers from the macular region enter the high-risk, inferior temporal region of the disc may have a higher risk of macular damage. Future work should test the hypothesis that patients with discs further above the middle line are more susceptible than those with lower discs.

Caveat

Our intention here was not to examine the prevalence of arcuate VF defects in the general populace or to determine the characteristics (such as gender, age, or diagnosis) of the subpopulation with these defects. However, it is important to assess the relative prevalence of macular defects, in general, and arcuate versus diffuse defects, in particular. Langerhorst et al.[5] found more glaucomatous damage on the 10-2 test than suspected on the 30-2 test in approximately 10% of their patients with suspected or very early glaucoma. Clearly the central 10° needs further study.

Summary

Arcuate defects of the RNFL produce a range of glaucomatous VF defects from those easily identified on the 24-2 test to those only seen on 10-2 tests. The defects seen on the 10-2 test can even include a papillofoveal horizontal step, or pistol barrel scotoma, in the temporal field, which is actually an arcuate region of damage on the RNFL. If RGC displacement is taken into consideration, the RNFL and VF defects can be compared directly. This should allow for improved presentation of fdOCT and VF information.

References

1. Stamper RL. The effect of glaucoma on central visual function. *Trans Am Ophthalmol Soc.* 1984;82:792–826.
2. Araie M. Pattern of visual field defect in normal-tension and high tension glaucoma. *Curr Opin Ophthalmol.* 1995;6:36–45.
3. Anctil J-L, Anderson DR. Early foveal involvement and generalized depression of the visual field in glaucoma. *Arch Ophthalmol.* 1984;102:363–370.
4. Koseki N, Araie M, Yamagami J, Suzuki Y. Sectorization of central 10-deg visual field in open-angle glaucoma. An approach for its brief evaluation. *Graefes Arch Clin Exp Ophthalmol.* 1995;233:621–626.
5. Langerhorst CT, Carenini LL, Bakker D, De Bie-Raakman MAC. Measurements for description of very early glaucomatous field defects. In: Wall M, Heiji A, eds. *Perimetry Update 1996/1997*. New York, NY: Kugler Publications; 1997:67–73.
6. Schiefer U, Papageorgiou E, Sample PA, et al. Spatial pattern of glaucomatous visual field loss obtained with regionally condensed stimulus arrangements. *Invest Ophthalmol Vis Sci.* 2010;51:5685–5689.
7. Sihota R, Gupta V, Tuli D, Sharma A, Sony P, Srinivasan G. Classifying patterns of localized glaucomatous visual field defects on automated perimetry. *J Glaucoma.* 2007;16:146–152.
8. Tan O, Chopra V, Lu AT, Schuman JS, et al. Detection of macular ganglion cell loss in glaucoma by Fourier-domain optical coherence tomography. *Ophthalmol.* 2009;116:2305–2314.
9. Wang M, Hood DC, Cho JS, et al. Measurement of local retinal ganglion cell layer thickness in patients with glaucoma using frequency-domain optical coherence tomography. *Arch Ophthalmol.* 2009;127:875–881.
10. Sakamoto A, Hangai M, Nukada M, et al. Three-dimensional imaging of macular retinal nerve fiber layer in glaucoma using spectral-domain optical coherence tomography. *Invest Ophthalmol Vis Sci.* 2010;51:5062–5070.
11. Hood DC, Thienprasiddhi P, Greenstein VC, et al. Detecting early to mild glaucomatous damage: a comparison of the multifocal VEP and automated perimetry. *Invest Ophthalmol Vis Sci.* 2004;45:492–498.
12. Hood DC, Zhang X, Greenstein VC, et al. An interocular comparison of the multifocal VEP: a possible technique for detecting local damage to the optic nerve. *Invest Ophthalmol Vis Sci.* 2000;41(6):1580–1587.
13. Hood DC, Greenstein VC. The multifocal VEP and ganglion cell damage: applications and limitations for the study of glaucoma. *Prog Retinal Eye Res.* 2003;22:201–251.
14. Graham SL, Klistorner AI, Grigg JR, et al. Objective VEP perimetry in glaucoma: asymmetry analysis to identify early deficits. *J Glaucoma.* 2000;9:10–19.
15. Goldberg I, Graham SL, Klistorner AI. Multifocal objective perimetry in the detection of glaucomatous field loss. *Am J Ophthalmol.* 2002;133:29–39.
16. Hood DC, Salant JA, Arthur SN, et al. The location of the inferior and superior temporal blood vessels and interindividual variability of the retinal nerve fiber layer thickness. *J Glaucoma.* 2010; [Epub ahead of print] PMID: 19661824.
17. Lichter PR, Henderson JW. Optic nerve infarction. *Trans Am Ophthalmol Soc.* 1977;75:103–121.
18. De Moraes CG, Prata TS, Liebmann CA, et al. Spatially consistent, localized visual field loss before and after disc hemorrhage. *Invest Ophthalmol Vis Sci.* 2009;50:4727–4733.
19. Lewis RA, Phelps CD. A comparison of visual field loss in primary open-angle glaucoma and the secondary glaucomas. *Ophthalmologica.* 1984;189:41–48.
20. Drasdo N, Millican CL, Katholi CR, Curcio CA. The length of Henle fibers in the human retina and a model of ganglion receptive field density in the visual field. *Vision Res.* 2007;47:2901–2911.
21. Nolan JM, Stringham JM, Beatty S, Snodderly DM. Spatial profile of macular pigment and its relationship to foveal architecture. *Invest Ophthalmol Vis Sci.* 2008;49:2134–2142.
22. Lefèvre F, Leroy K, Delrieu B, Lassale D, Péchereau A. Study of the optic nerve head-fovea angle with retinophotography in healthy patients. *J Fr Ophtalmol.* 2007;30:598–606.
23. Rohrschneider K. Determination of the location of the fovea on the fundus. *Invest Ophthalmol Vis Sci.* 2004;45:3257–3258.
24. Garway-Heath DF, Poinoosawmy D, Fitzke FW, Hitchings RA. Mapping the visual field to the optic disc in normal tension glaucoma eyes. *Ophthalmol.* 2000;107:1809–1815.
25. Hood DC, Anderson SC, Wall M, Kardon RH. Structure versus function in glaucoma: An application of a linear model. *Invest Ophthalmol Vis Sci.* 2007;48:3662–3668.
26. Kanadani FN, Hood DC, Grippo TM, et al. Structural and functional assessment of the macular region in patients with glaucoma. *Br J Ophthalmol.* 2006;90:1393–1397.